Recent Developments of Transmissive Reconfigurable Intelligent Surfaces: A Review

TANG Junwen, XU Shenheng, YANG Fan, LI Maokun
(Department of Electronic Engineering, Tsinghua University, Beijing 100084, China)

DOI: 10.12142/ZTECOM.202201004
https://kns.cnki.net/kcms/detail/34.1294.TN.20220305.1951.004.html, published online March 8, 2022
Manuscript received: 2022-01-24

Abstract: Reconfigurable intelligent surface (RIS) is considered as one of the key technologies for the next-generation mobile communication systems. The transmissive RIS is able to achieve dynamic beamforming capability while transmitting an in-band RF signal through its aperture, and has promising prospects in various practical application scenarios. This paper reviews some of the latest developments of the transmissive RIS. The approaches for transmissive RIS designs are classified and described briefly. Numerous designs with different phase resolutions, such as 1-bit, 2-bit or continuous 360° phase shifts, are presented, with detailed discussions on their operating mechanisms and transmission performances. The design solutions for various transmissive RIS elements are summarized and compared.

Keywords: antenna; mobile communications; phase shifter; RIS; transmitarray

Citation (IEEE Format): J. W. Tang, S. H. Xu, F. Yang, et al, "Recent developments of transmissive reconfigurable intelligent surfaces: a review, " *ZTE Communications*, vol. 20, no. 1, pp. 21 – 27, Mar. 2022. doi: 10.12142/ZTECOM.202201004.

1 Introduction

As one of the key technologies for the next-generation mobile communication systems, the reconfigurable intelligent surface (RIS) [1–3] has attracted great attentions recently. On the contrary to the commonly used reflection mode, the transmissive RIS is able to achieve dynamic beamforming capability while transmitting an in-band RF signal through its aperture. This distinctive feature allows much improved direct indoor coverage by the outdoor cellular signals. It can also be employed as a reconfigurable radome for 5G base station antennas or terminal antennas. The large-scale RIS array can effectively boost the coverage of the medium-sized 5G massive multiple-input multiple-output (MIMO) antennas, and the analog-digital hybrid structure can keep the overall cost and power consumption low.

Solid-state electronic devices are commonly integrated in each constituent RIS element to achieve phase reconfigurability. Continuous phase shifts can be realized using analog-type devices like varactor diodes[4–13]. The phase shift range usually exceeds 360° so that the phase errors are negligible. However, the transmission insertion loss of the RIS element is relatively high and for instance, can be up to 5.7 dB[7], considerably reducing the aperture efficiency of the RIS. Switch-type devices, such as p-i-n diodes and radio frequency (RF) microelectromechanical system (MEMS) switches, are widely used to produce discrete phase shifts[14–31], especially at millimeter wave frequencies. Most designs focus on 1-bit phase reconfigurability because the complexity in design and fabrication is more manageable[14–27]. The phase quantization errors associated with discrete phase shifts inevitably introduce performance degradation[32–34]. It is observed that the 1-bit designs suffer from 3 – 4 dB loss attributed to the coarse phase resolution, resulting in low aperture efficiencies. The sidelobe levels are usually much higher, sometimes even causing unwanted grating lobes. The 2-bit design is considered a well-balanced choice between the design complexity and the element performance. The phase quantization loss can be greatly reduced to less than 1 dB, and the sidelobe envelop is much improved as well[28–31].

Most transmissive RIS designs are based on the receiver-transmitter (Rx-Tx) structure[4–9, 14–22, 25–31], and microstrip patch antennas[4–9, 14–18, 20–21, 25–26, 30], slot antennas[19, 28–29], vivaldi antennas[22] and dipole antennas[27, 31] are employed as receivers or transmitters. There are a handful of designs using the stacked frequency selective surface (FSS) structures[10–13, 23–24]. Each FSS layer provides a finite-degree phase shift, and a wide phase shift range is achieved by stacking multiple FSS layers. The structure is relatively more complicated and more solid-state electronic devices are needed in each unit cell.

This paper provides a review of some recent transmissive

RIS studies and is organized as follows. The configuration classification of the transmissive RIS is introduced in Section 2. Various transmissive RIS designs with different phase resolutions or polarizations are described in Section 3. Finally, conclusions are given in Section 4.

2 Design Approaches

There are two widely used design approaches for the transmissive RIS, which are the receiver-transmitter (Rx-Tx) structure and the stacked FSS structure. Generally, a typical Rx-Tx structure consists of three components: the receiving (Rx) cell, the transmitting (Tx) cell, and the power transmission structure. A ground plane separates the Rx from the Tx, so that they can operate independently, avoiding the mutual interference with each other. The power transmission structure between them is usually realized by a metallic via[7–9, 14–18, 20–21, 25–27, 30] or a slot-coupling structure[4–6]. When the RIS is illuminated by an incident wave, the Rx on one side of the RIS first receives the wave and converts it into a guided wave. This wave is then conveyed through the power transmission structure to the Tx deployed on the other side of the RIS, and re-radiated to the free space. The phase shift can be realized on either the Rx, the Tx, or the power transmission structure.

The stacked FSS structure type is inspired by the classic FSS designs. It consists of multiple FSS layers of metallic and dielectric substrates. A phase shift with finite degrees is obtained when a wave propagates through each FSS layer, and by cascading multiple layers, a larger phase shift can usually be realized. The separation between layers is also a crucial parameter. The overall thickness is relatively large. Unlike the Rx-Tx type, there is no ground plane in the stacked FSS structure type (Fig. 1).

3 Representative Transmissive RIS Designs

3.1 Single-Polarized 1-Bit Designs

A 1-bit transmissive RIS element can realize two phase states with a phase difference of 180°. Generally, there are two operating mechanisms in the element designs, which are the current reversal method and the variable resonance method. The current reversal method based on the Rx-Tx structure is most popular for 1-bit designs in literature. The p-i-n diode is usually chosen as the controlling device due to its small volume and stable performance especially at high frequencies. The p-i-n diode can work at "ON" or "OFF" states by supplying a different DC biasing signal. In practice, two p-i-n diodes are usually embedded in parallel and in opposite directions in each element, and a single positive or negative biasing signal can switch them between the "ON-OFF" and "OFF-ON" states. Hence, the excitation current on the radiating element flows in opposite directions, and the radiated field is reversed, resulting in a stable phase shift of 180°. The stacked FSS type structure is usually based on the variable resonance method. The resonant characteristic of the element structure is manipulated by switching the integrated p-i-n diode "ON" or "OFF", and consequently, a phase difference in its radiated field is caused. It is noted that the phase difference varies with frequency, and its bandwidth is usually narrower than that using the current reversal method.

Single polarized 1-bit RIS has been widely investigated. A representative linearly polarized design with an O-slot patch and two p-i-n diodes based on the Rx-Tx structure and the current reversal mechanism is proposed in Ref. [14], as shown in Fig. 2(a). The element evolves from the U-slot microstrip patch antenna. It is modified into an O-slot so that two p-i-n diodes placed across it and biased in opposite states can effectively form a U-slot patch with reversible direction, thereby achieving a phase difference of 180° due the current reversal mechanism. A metallic via connecting the Rx and the Tx is used to transmit the signal from the incident side to the re-radiating side. The measured transmission insertion loss is 1.7/1.9 dB for two states and the 3-dB transmission bandwidth is 14.7%. Moreover, the DC biasing circuit is elaborately designed. The positive end of one p-i-n diode and the negative end of the other are connected together through two symmetrical metallic vias. Only a single DC biasing signal is required

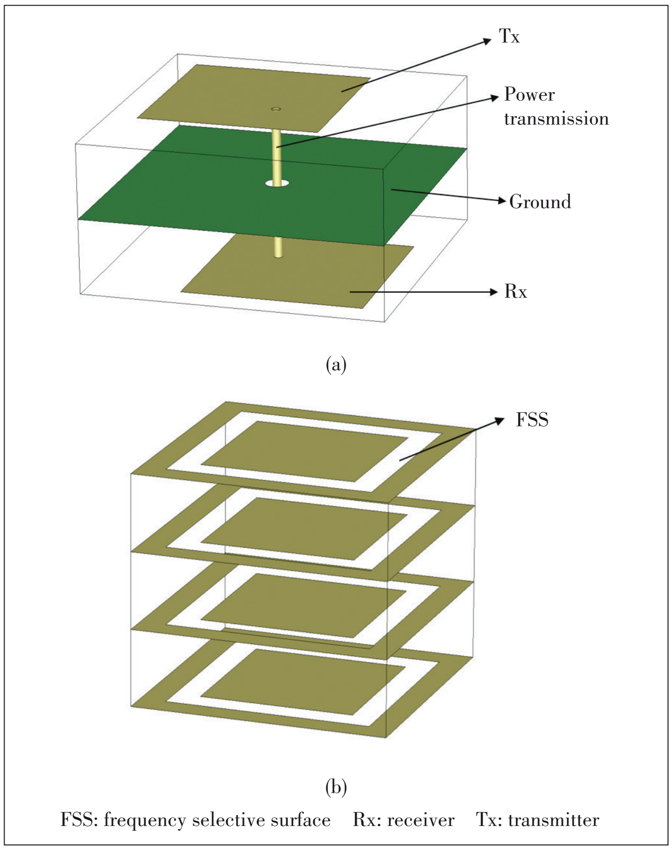

▲ Figure 1. Design approaches: (a) Rx-Tx structure; (b) stacked FSS structure

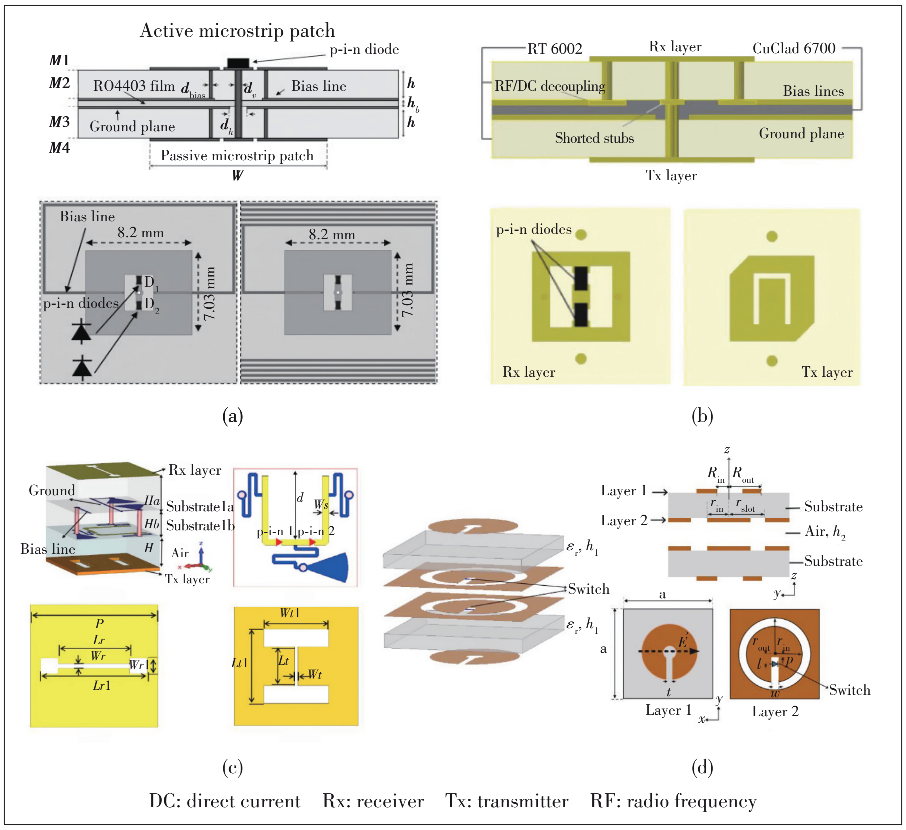

▲ Figure 2. Schematics of single-polarized 1-bit transmissive reconfigurable intelligent surface (RIS) elements: (a) linear polarization in Ref. [14]; (b) linear-circular polarization conversion in Ref. [16]; (c) slot coupling structure in Ref. [19]; (d) variable resonance design in Ref. [23]

to control them working at opposite states. The biasing lines are arranged close to the ground, thus minimizing its interference on the RF performance. It is also worth mentioning that by truncating the corners of the U-slot patch or modifying the U-slot patch, the 1-bit linearly polarized element can be readily developed into a single linear-circular polarization conversion[16, 18] or polarization switching designs[17]. The sketch of the element in Ref. [16] is shown in Fig. 2(b). A minimum transmission insertion loss of 1.59/1.70 dB at Ka band with a 3-dB bandwidth of more than 12% is validated in measurement.

The 1-bit element presented in Ref. [19] exploits two slot antennas as Rx and Tx. As Fig. 2(c) shows, two H-shaped slots are placed orthogonally to receive and re-radiate electromagnetic waves, with high polarization isolation due to the polarization orthogonality. Two p-i-n diodes are integrated in the U-shaped transmission line to control the excitation current direction. By switching them working at “ON-OFF” or “OFF-ON” state, the electric field coupled to the Tx H-slot is reversed, resulting in a 180° phase shift. The operating frequency of the element is 12.5 GHz, and the simulated transmission insertion loss is 0.86/0.76 dB.

A 1-bit element design based on the variable resonance method is proposed in Ref. [23], and the element configuration is shown in Fig. 2(d). It is composed of four metallic layers and two layers of dielectric substrates. The upper and lower C-shaped patches are utilized for the transmission of the electromagnetic waves, with two ring slots loaded by a rectangular gap used as the phase shifter. Two p-i-n diodes are positioned across the two rectangular gaps and work at “ON-ON” or “OFF-OFF” state. They change the widths of the gaps, and consequently, the equivalent resonance length varies, thus shifting the transmission phase of the element. The measurement shows that the element transmission insertion losses for the two phase states at 11.5 GHz are 0.6 dB and 2.9 dB, respectively. Note that the transmission insertion loss increases due to the detuning of the resonant characteristic of the element structure when the 180° phase shift is realized.

3.2 Dual-Polarized 1-Bit Designs

The dual-polarized transmissive RIS designs mostly focus on 1-bit phase resolution. In general, there are two solutions. One is to excite two orthogonal radiating modes of the same radiator[25], and the other is to arrange two sets of single-polarized 1-bit RIS elements orthogonally to achieve the dual-polarized function[24, 26–27]. Note that there are some designs with the polarization manipulation capability[7, 17–18]; however, they are unable to operate in two polarization directions simultaneously and hence excluded in this section.

The dual-linear polarized 1-bit element proposed in Ref. [25] exploits a five-layer-stacked configuration. The element configuration is illustrated in Fig. 3(a). For the realization of the single-linear polarized 1-bit phase controlling, it relies on the U-shaped feeding line integrated with two p-i-n diodes. By alternatively switching the working states, the radiated fields in opposite direction are excited on the top metallic square ring, and a 180° phase difference can be generated. A dual-linear polarized design can be achieved by employing two orthogonally placed U-shaped feeding lines to excite the same metallic square ring. The measured results show that this element can achieve a transmission insertion loss of 1.7/1.9 dB at 5.9 GHz, with an operating bandwidth of 2.8%.

Ref. [27] presents a dual-linear polarized 1-bit RIS element based on a via-fed dipole with a parasitic dipole. Fig. 3(b) describes the fundamental single-polarized 1-bit RIS element. The element employs the Rx-Tx structure, both based on di-

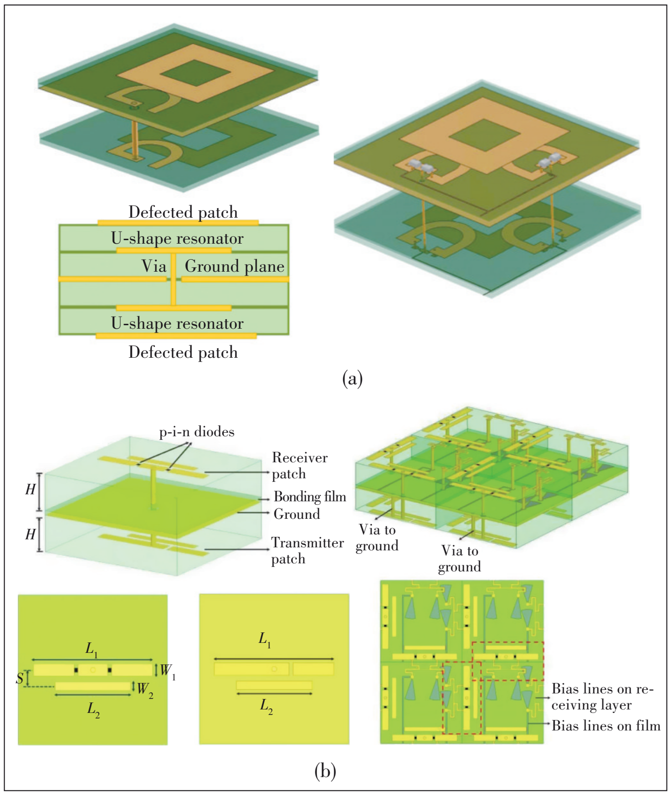

▲**Figure 3. Schematics of the dual-linear polarized 1-bit transmissive reconfigurable intelligent surface (RIS) element designs: (a) two orthogonal radiating modes of the same radiator in Ref. [25]; (b) two sets of via-fed dipoles with parasitic dipoles in Ref. [27]**

pole configurations. Two p-i-n diodes are placed on the arms of the receiver dipole, and a parasitic dipole is added near the dipole to reduce the loss. The mechanism can be explained as the current is mostly coupled to the parasitic dipole, reducing the loss that is caused by the current flowing through the p-i-n diodes. Therefore, the simulated element transmission insertion loss is only 0.8 dB at 12.25 GHz. The design of the dual-linear polarized element can be accomplished by arranging two sets of single-linear polarized elements orthogonally.

3.3 2-Bit Designs

Although considerable developments of the 1-bit transmissive RIS designs have been accomplished, they still suffer from suboptimal radiation behavior caused by the large phase quantization error. In order to increase the phase accuracy so as to improve the radiation performance, the 2-bit design is investigated.

Another 2-bit RIS element at Ka band is proposed in Refs. [28–29]. As illustrated in Fig. 4(a), the Rx and Tx slots are fed with striplines, and five RF MEMS switches are loaded on the striplines to switch the four operating modes alternatively. The measured element transmission insertion loss, however, reaches up to 4.2–9.2 dB due to the challenging fabrication process. A Ka-band linearly polarized 2-bit RIS element is presented in Ref. [30]. The configuration of the element is depicted in Fig. 4(b). It is composed of six metallic layers and three dielectric substrates, with four integrated p-i-n diodes. The 180° phase shift is realized by alternating the two p-i-n diodes loaded on the receiving O-slot patch. Two more p-i-n diodes are loaded on the transmitting patch, which contains a delay line to achieve the additional 0°/90° phase switching. Thus, the 2-bit phase tuning capability can be obtained. The measured element insertion loss is 1.5 – 2.3 dB for the four phase states at 29 GHz, with the measured 3-dB transmission bandwidth of 10.1% – 12.1%.

3.4 Designs with Continuous Phase Shift

To achieve a continuous 360° phase shift, varactor diodes

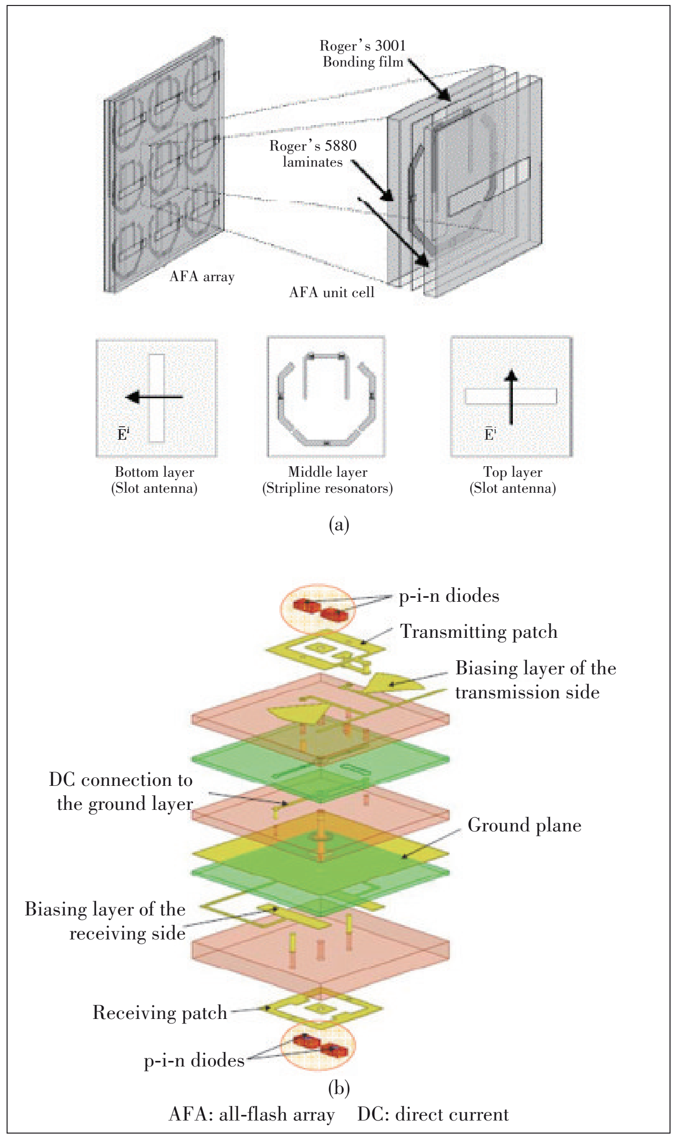

▲ **Figure 4. Schematics of the 2-bit transmissive reconfigurable intelligent surface (RIS) element designs: (a) dual polarization with five radio frequency (RF) microelectromechanical system (MEMS) switches in Refs. [28–29]; (b) O-slot patches loaded with four p-i-n diodes in Ref. [30]**

are widely utilized in most transmissive RIS element designs since the capacitance of the varactor diodes can be changed by applying a DC biasing voltage. One phase tuning approach is based on the microstrip phase shifter[4–5, 7–9]. By employing the Rx-Tx structure, the varactor diodes are placed on the phase shifter to control the transmission phase, ensuring the stability of the transmission insertion loss in the operating frequency band when the DC biasing voltage changes. Thus, most wideband RIS designs explore this approach to tune phase shift. The other approach is to change the resonant characteristic of the element structure[6, 10–13], and it is widely used in the stacked FSS structures.

An element with continuous phase controlling can be found in Ref. [5], and the element structure is exhibited in Fig. 5(a).

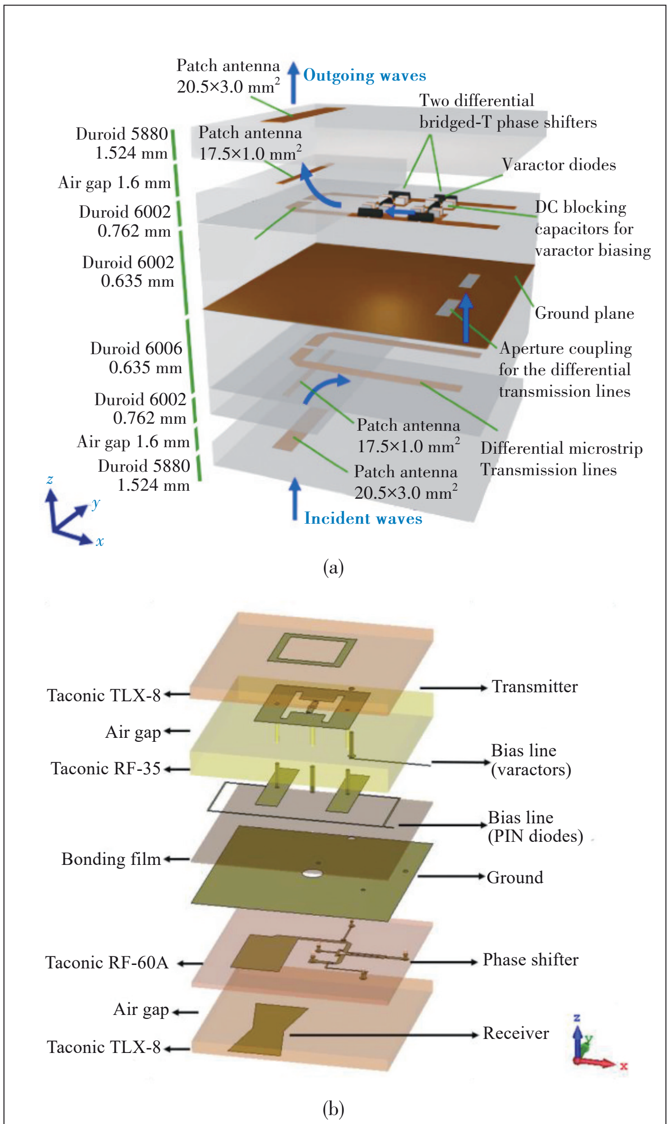

▲ **Figure 5. Transmissive reconfigurable intelligent surface (RIS) element designs with 360° phase controlling: (a) two cascaded bridged-T phase shifters in Ref. [5]; (b) a 180° analog phase shifter combined with 1-bit phase shifter in Ref. [9]**

The microstrip-slot coupling structure is adopted in this design to transfer energy between Rx and Tx, which are both stacked dipole patches. Two cascaded bridged-T phase shifters loaded with six varactor diodes are selected to reconstruct the transmission phase. It is worth mentioning that the stacked dipole patches are fed by the differential microstrip transmission lines, and two rectangular gaps are opened in the ground to transfer the differential signals. The simulated results demonstrate that the element is capable of a phase tuning range of over 400°, with the transmission loss maintaining below 3.6 dB.

Some attempts have been done in Ref. [9] to reduce the element transmission insertion loss, and the schematic of the proposed element is displayed in Fig. 5(b). By combining a 180° analog phase shifter loaded with varactor diodes and a 1-bit phase shifter loaded with p-i-n diodes, the element is able to shift its transmission phase over 360°. By utilizing the simple current reversal mechanism, the 1-bit phase shifter circuit is integrated with the Tx patch instead of using a complex phase shifter, and the element insertion loss is effectively reduced. It is indicated that the simulated transmission insertion loss ranges from 0.95 dB to 1.35 dB at 5.6 GHz, with a 3-dB transmission loss bandwidth of 16.7%.

In Ref. [6], an element consisting of three resonant structures is exhibited. As displayed in Fig. 6(a), two microstrip patches embedded with varactor diodes operate as two resonant structures. They are positioned on the two sides of a ground plane and coupled by a slot aperture. A varactor diode is inserted into the slot to form the third resonant structure. Therefore, the resonant frequency of the radiating patch could be manipulated by changing the biasing voltages applied on the varactor diodes. The measured phase shift ranges at 5.5 GHz is only 245° while the transmission insertion loss reaches up to 2.7 – 5.7 dB.

Based on the stacked FSS structure, a continuous phase controlling RIS element at C band is detailed in Ref. [13]. As illustrated in Fig. 6(b), it is made of a five-layer stacked square slot and an extra layer to accommodate the biasing circuits. Each square slot FSS is loaded with two surface-mounted device (SMD) varactors and functions as a band-pass filter. This means if the frequency of the incident wave is close to the resonant frequency of the FSS, it can propagate through FSS. By adjusting the values of the SMD varactors, the resonant frequency of the square slot varies, and thus the phase response of the propagating wave can be controlled. Thanks to the cumulative effects of the phase response of each FSS, the stacked FSS element can generate a phase tuning range of 360° when the transmission insertion loss is within 3 dB in simulations. However, the operating bandwidth is only 90 MHz.

4 Conclusions

Recently, the RIS technology develops rapidly as the demands of low-cost and low power consumption beamforming systems increase. Various application scenarios of the RIS

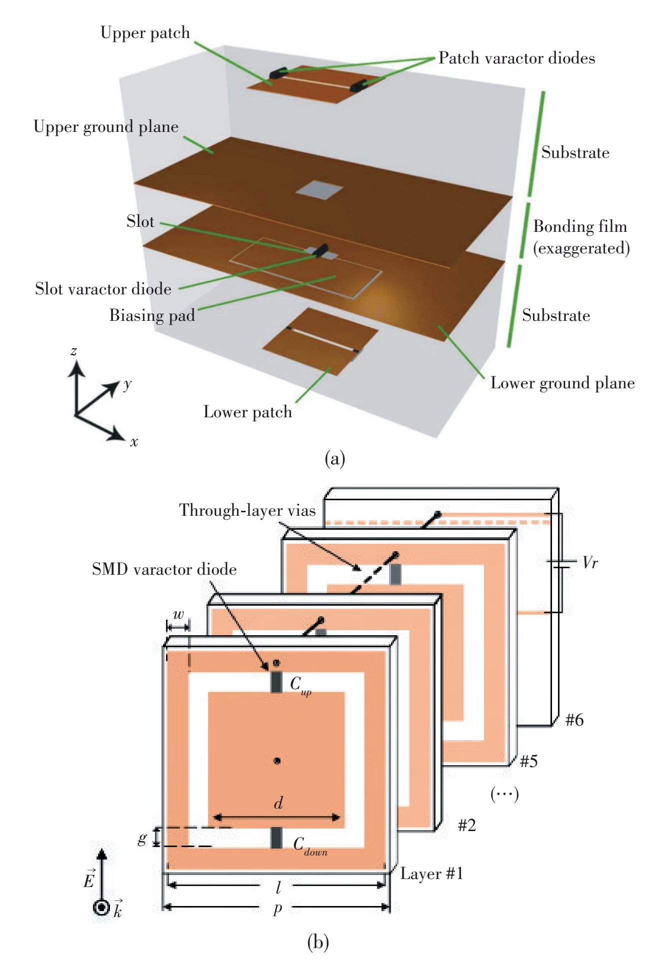

▲ **Figure 6. Transmissive reconfigurable intelligent surface (RIS) element designs with 360° phase controlling: (a) an element with three resonant structures in Ref. [6]; (b) 5-layer stacked frequency selective surface (FSS) structure in Ref. [13]**

have been explored, such as wireless power delivery[35], wireless coverage extension[36] and efficient channel estimation[37]. Specifically, the transimissive RIS has found its place in the indoor signal coverage. This paper reviews some of the latest developments of the transmissive RIS designs. The design methods utilized in most transmissive RIS designs are briefly introduced. Several representative designs with different phase resolution and polarization capabilities are presented and discussed. Currently, great efforts are being made to push the frequency frontier of the RIS technology towards the W and THz bands. Active devices are being incorporated to achieve signal boosting capability. Various RIS-aided systems are being developed to demonstrate the potential applications of the RIS technology in future wireless communications. It is believed that the RIS has a promising future.

References

[1] LIASKOS C, NIE S, TSIOLIARIDOU A, et al. A new wireless communication paradigm through software-controlled metasurfaces [J]. IEEE communications magazine, 2018, 56(9): 162 – 169. DOI: 10.1109/MCOM.2018.1700659
[2] TANG W, LI X, DAI J, et al. Wireless communications with programmable metasurface: transceiver design and experimental results [J]. China communications, 2019, 16(5): 46 – 61. DOI: 10.23919/J.CC.2019.05.004
[3] DAI L, WANG B, WANG M, et al. Reconfigurable intelligent surface-based wireless communications: antenna design, prototyping, and experimental results [J]. IEEE access, 2020, 8: 45913 – 45923. DOI: 10.1109/ACCESS.2020.2977772
[4] LAU J Y, HUM S V. A wideband reconfigurable transmitarray element [J]. IEEE transactions on antennas and propagation, 2011, 60(3): 1303 – 1311. DOI: 10.1109/TAP.2011.2180475
[5] LAU J Y, HUM S V. Reconfigurable transmitarray design approaches for beamforming applications [J]. IEEE transactions on antennas and propagation, 2012, 60(12): 5679 – 5689. DOI: 10.1109/TAP.2012.2213054
[6] LAU J Y, HUM S V. Analysis and characterization of a multipole reconfigurable transmitarray element [J]. IEEE transactions on antennas and propagation, 2010, 59(1): 70 – 79. DOI: 10.1109/TAP.2010.2090456
[7] HUANG C, PAN W, MA X, et al. Using reconfigurable transmitarray to achieve beam-steering and polarization manipulation applications [J]. IEEE transactions on antennas and propagation, 2015, 63(11): 4801 – 4810. DOI: 10.1109/TAP.2015.2479648
[8] HUANG C, PAN W, LUO X. Low-loss circularly polarized transmitarray for beam steering application [J]. IEEE transactions on antennas and propagation, 2016, 64(10): 4471 – 4476. DOI: 10.1109/TAP.2016.2586580
[9] TANG J, XU S, YANG F, et al. Design and measurement of a reconfigurable transmitarray antenna with compact varactor-based phase shifters [J]. IEEE antennas and wireless propagation letters, 2021, 20(10): 1998 – 2002. DOI: 10.1109/LAWP.2021.3101891
[10] FRANK M, LURZ F, WEIGEL R, et al. Electronically reconfigurable 6× 6 element transmitarray at K-band based on unit cells with continuous phase range [J]. IEEE antennas and wireless propagation letters, 2019, 18(4): 796 – 800. DOI: 10.1109/LAWP.2019.2903338
[11] BOCCIA L, RUSSO I, AMENDOLA G, et al. Multilayer antenna-filter antenna for beam-steering transmit-array applications [J]. IEEE transactions on microwave theory and techniques, 2012, 60(7): 2287 – 2300. DOI: 10.1109/TMTT.2012.2195673
[12] REIS J R, COPNER N, HAMMOUDEH A, et al. FSS-inspired transmitarray for two-dimensional antenna beamsteering [J]. IEEE transactions on antennas and propagation, 2016, 64(6): 2197 – 2206. DOI: 10.1109/TAP.2016.2543802
[13] REIS J R, CALDEIRINHA R F S, HAMMOUDEH A, et al. Electronically reconfigurable FSS-inspired transmitarray for 2-D beamsteering [J]. IEEE transactions on antennas and propagation, 2017, 65(9): 4880 – 4885. DOI: 10.1109/TAP.2017.2723087
[14] CLEMENTE A, DUSSOPT L, SAULEAU R, et al. 1-bit reconfigurable unit cell based on PIN diodes for transmit-array applications in X-band [J]. IEEE transactions on antennas and propagation, 2012, 60(5): 2260 – 2269. DOI: 10.1109/TAP.2012.2189716
[15] CLEMENTE A, DUSSOPT L, SAULEAU R, et al. Wideband 400-element electronically reconfigurable transmitarray in X band [J]. IEEE transactions on antennas and propagation, 2013, 61(10): 5017 – 5027. DOI: 10.1109/TAP.2013.2271493
[16] DI PALMA L, CLEMENTE A, DUSSOPT L, et al. Experimental characterization of a circularly polarized 1 bit unit cell for beam steerable transmitarrays at Ka-band [J]. IEEE transactions on antennas and propagation, 2018, 67(2): 1300 – 1305. DOI: 10.1109/TAP.2018.2880095
[17] PAN W, HUANG C, MA X, et al. A dual linearly polarized transmitarray element with 1-bit phase resolution in X-band [J]. IEEE antennas and wireless propagation letters, 2014, 14: 167 – 170. DOI: 10.1109/LAWP.2014.2358267
[18] HUANG C, PAN W, MA X, et al. 1-bit reconfigurable circularly polarized transmitarray in X-band [J]. IEEE antennas and wireless propagation letters, 2015, 15: 448 – 451. DOI: 10.1109/LAWP.2015.2451697
[19] WANG M, XU S, YANG F, et al. Design and measurement of a 1-bit reconfigurable transmitarray with subwavelength H-shaped coupling slot elements [J]. IEEE transactions on antennas and propagation, 2019, 67(5): 3500 – 3504.

DOI: 10.1109/TAP.2019.2902676

[20] WANG Y, XU S, YANG F, et al. A novel 1 bit wide-angle beam scanning reconfigurable transmitarray antenna using an equivalent magnetic dipole element [J]. IEEE transactions on antennas and propagation, 2020, 68(7): 5691 – 5695. DOI: 10.1109/TAP.2020.2964954

[21] WANG M, XU S, YANG F, et al. A novel 1-bit reconfigurable transmitarray antenna using a C-shaped probe-fed patch element with broadened bandwidth and enhanced efficiency [J]. IEEE access, 2020, 8: 120124 – 120133. DOI: 10.1109/ACCESS.2020.3004435

[22] XIAO Y, YANG F, XU S, et al. Design and implementation of a wideband 1-bit transmitarray based on a yagi-vivaldi unit cell [J]. IEEE transactions on antennas and propagation, 2021 69(7): 4229 – 4234. DOI: 10.1109/TAP.2020.3048496

[23] NGUYEN B D, PICHOT C. Unit-cell loaded with PIN diodes for 1-bit linearly polarized reconfigurable transmitarrays [J]. IEEE antennas and wireless propagation letters, 2018, 18(1): 98 – 102. DOI: 10.1109/LAWP.2018.2881555

[24] WANG M, XU S, YANG F, et al. A novel 1-bit dual-linear polarized reconfigurable transmitarray element using double-layer dipoles [C]//IEEE Asia-Pacific Microwave Conference (APMC). IEEE, 2019: 685 – 687. DOI: 10.1109/APMC46564.2019.9038225

[25] MUNINA I, TURALCHUK P, VEREVKIN A, et al. A study of C-band 1-bit reconfigurable dual-polarized transmitarray [C]//13th European Conference on Antennas and Propagation (EuCAP). EurAAP, 2019: 1 – 5

[26] PHAM K, SAULEAU R, CLEMENTE A, et al. Electronically reconfigurable unit-cell and transmitarray in dual-linear polarization at Ka-band [C]//13th European Conference on Antennas and Propagation (EuCAP). EurAAP, 2019: 1 – 4

[27] WANG Y, XU S, YANG F, et al. 1 bit dual-linear polarized reconfigurable transmitarray antenna using asymmetric dipole elements with parasitic bypass dipoles [J]. IEEE transactions on antennas and propagation, 2021, 69(2): 1188 – 1192. DOI: 10.1109/TAP.2020.3005713

[28] CHENG C C, ABBASPOUR-TAMIJANI A. Study of 2-bit antenna-filter-antenna elements for reconfigurable millimeter-wave lens arrays [J]. IEEE transactions on microwave theory and techniques, 2006, 54(12): 4498 – 4506. DOI: 10.1109/TMTT.2006.885993

[29] CHENG C C, LAKSHMINARAYANAN B, ABBASPOUR-TAMIJANI A. A programmable lens-array antenna with monolithically integrated MEMS switches [J]. IEEE transactions on microwave theory and techniques, 2009, 57 (8): 1874 – 1884. DOI: 10.1109/TMTT.2009.2025422

[30] DIABY F, CLEMENTE A, DI PALMA L, et al. Design of a 2-bit unit-cell for electronically reconfigurable transmitarrays at Ka-band [C]//47th European Microwave Conference (EuMC). EuMA, 2017: 1321 – 1324. DOI: 10.23919/EuMC.2017.8231095

[31] TANG J, XU S, YANG F. Design of a 2.5-D 2-bit reconfigurable transmitarray element for 5G mmwave applications [C]//IEEE International Symposium on Antennas and Propagation and North American Radio Science Meeting. IEEE, 2020: 631 – 632. DOI: 10.1109/IEEECONF35879.2020.9330153

[32] WU B, SUTINJO A, POTTER M E, et al. On the selection of the number of bits to control a dynamic digital MEMS reflectarray [J]. IEEE antennas and wireless propagation letters, 2008, 7: 183 – 186. DOI: 10.1109/LAWP.2008.920908

[33] YANG H, YANG F, XU S, et al. A study of phase quantization effects for reconfigurable reflectarray antennas [J]. IEEE antennas and wireless propagation letters, 2017, 16: 302 – 305. DOI: 10.1109/LAWP.2016.2574118

[34] WU Q, ZHANG R. Beamforming optimization for wireless network aided by intelligent reflecting surface with discrete phase shifts [J]. IEEE transactions on communications, 2020, 68(3): 1838 – 1851. DOI: 10.1109/TCOMM.2019.2958916

[35] BUCKMASTER J G, LEE T H. An electronically steerable millimeter-wave reflectarray for wireless power delivery [C]//50th European Microwave Conference (EuMC). EuMA, 2021: 514 – 517. DOI: 10.23919/EuMC48046.2021.9338208

[36] ZENG S, ZHANG H, DI B, et al. Reconfigurable intelligent surface (RIS) assisted wireless coverage extension: RIS orientation and location optimization [J]. Communications letters, 2020, 25(1): 269 – 273. DOI: 10.1109/LCOMM.2020.3025345

[37] MILLER C L, DMOCHOWSKI P A, SMITH P J. Efficient channel estimation for RIS [C]//IEEE International Conference on Communications. IEEE, 2021: 1 – 6. DOI: 10.1109/ICC42927.2021.9500469

Biographies

TANG Junwen (tjw17@mails.tsinghua.edu.cn) received the B.S. degree in electronic information engineering from Xidian University, China in 2017, and she is currently pursuing the Ph.D. degree at Department of Electronic Engineering, Tsinghua University, China. Her current research interests include antenna theory and reconfigurable antenna.

XU Shenheng (shxu@tsinghua.edu.cn) received the B.S. and M.S. degrees from Southeast University, China in 2001 and 2004, respectively and the Ph.D. degree in electrical engineering from the University of California at Los Angeles (UCLA), USA in 2009. From 2000 to 2004, he was a research assistant with the State Key Laboratory of Millimeter Waves, Southeast University, China. From 2004 to 2011, he was a graduate student researcher and then became a postdoctoral researcher with the Antenna Research, Analysis, and Measurement Laboratory, UCLA. In 2012, he joined the Department of Electronic Engineering, Tsinghua University, China, as an associate professor. His current research interests include novel designs of high-gain antennas for advanced applications, artificial electromagnetic structures, and electromagnetic and antenna theories.

YANG Fan received the B.S. and M.S. degrees from Tsinghua University, China and the Ph.D. degree from the University of California at Los Angeles (UCLA), USA. He joined the Electrical Engineering Department, University of Mississippi, USA, as an assistant professor and was promoted to an associate professor in 2009. In 2011, he joined the Electronic Engineering Department, Tsinghua University, as a professor. He has authored or coauthored more than 300 journal articles and conference articles, six book chapters, and five books. Dr. YANG is an ACES Fellow, IEEE Fellow, and a recipient of several prestigious awards and recognition, including the Young Scientist Awards of the 2005 URSI General Assembly and of the 2007 International Symposium on Electromagnetic Theory, the 2008 Junior Faculty Research Award of the University of Mississippi, the 2009 Inaugural IEEE Donald G. Dudley Jr. Undergraduate Teaching Award, and the 2011 Recipient of Global Experts Program of China. He was the Technical Program Committee (TPC) Chair of 2014 IEEE International Symposium on Antennas and Propagation and USNC-URSI Radio Science Meeting. He is also an IEEE APS Distinguished Lecturer from 2018 to 2020. His current research interests include antennas, surface electromagnetics, computational electromagnetics and applied electromagnetic systems.

LI Maokun received the B.S. degree in electronic engineering from Tsinghua University, China in 2002, and the M.S. and Ph.D. degrees in electrical engineering from the University of Illinois at Urbana-Champaign, USA in 2004 and 2007, respectively. After graduation, he worked as a senior research scientist at Schlumberger-Doll Research, USA. Since 2014, he has joined the Department of Electronic Engineering, Tsinghua University. He has authored one book chapter, 50 journal articles and 120 conference proceedings, and held three patent applications. His research interests include fast algorithms in computational electromagnetics and their applications in antenna modeling, electromagnetic compatibility analysis, and inverse problems. Dr. LI was a recipient of the China National 1 000 Plan in 2014 and the 2017 IEEE Ulrich L. Rohde Innovative Conference Paper Award. He also serves as the Associate Editor for the *IEEE Journal on Multiscale and Multiphysics Computational Techniques* and *Applied Computational Electromagnetic Society Journal*, and the Guest Editor for the special issue on “Electromagnetic Inverse Problems for Sensing and Imaging” in *IEEE Antennas and Propagation Magazine*.